Paratropic Delocalized Ring Currents in Flattened Cyclooctatetraene Systems with Bond Alternation**

Patrick W. Fowler, Remco W. A. Havenith, Leonardus W. Jenneskens,* Alessandro Soncini, and Erich Steiner

The classical Hückel and London theories of monocyclic π systems lead to an expectation of *diatropic* and *paratropic* ring currents in cycles with $4n + 2$ and $4n$ π electrons, respectively.[1] In practice, benzene famously bears out this expectation,[2, 3] but the 8π-antiaromatic cyclooctatetraene (COT) distorts to achieve a nonplanar closed-shell configuration with localized double bonds,[4] and behaves chemically as a conjugated alkene.[5]

Synthetic chemists have shown an interest in using annelation with rigid bridges to impose geometric constraints to localize the electronic structure of benzene[6–9] and, conversely, to impose a delocalized structure on COT.[10, 11] The recent synthesis of a stable annelated cyclooctatetraene, tetrakis-(bicyclo[2.1.1]hexeno)cyclooctatetraene (**1**, Scheme 1),[11] in which the eight-membered ring is confined to the plane but retains strong bond alternation (X-ray average; $\Delta R(\mathbf{1}) = 0.169$ Å[11]), raises the question of whether this molecule will now follow the original Hückel–London expectation and, in spite of its bond alternation,[12] support a delocalized paratropic ring current. The positive nucleus-independent chemical shift (NICS)[13] value of $\delta = 10.6$ ppm calculated for the octagonal ring, though much smaller than that for planar COT (**2**(D_{4h}) $\delta = 27.2$ ppm),[11] is one indication of such a current. Unfortunately, **1** does not have the protons attached to its planar COT ring that would allow direct diagnosis by ^{1}H NMR spectroscopy, whilst its bridgehead protons lie outside the shielding/deshielding cone of the central ring. (In fact, the remoteness of the bridgehead protons explains the small size of the observed shift of $\delta = 0.18$ ppm,[6, 11] despite reversal of ring currents, between **1** and tris(bicyclo[2.1.1]hexeno)benzene; the ^{1}H NMR chemical shifts of bridgehead protons are similar in several bicyclo[2.1.1]hexeno-clamped derivatives of benzene and COT.[6, 11, 14, 15]).

Here we use computed current–density maps to answer the question of whether **1** supports a delocalized paratropic ring current. Consideration of the maps leads to a general analysis of the factors that decide when a constrained ring will carry a

[*] Prof. Dr. L. W. Jenneskens
Debye Institute, Department of Physical Organic Chemistry
Utrecht University
Padualaan 8, 3584 CH Utrecht (The Netherlands)
Fax: (+31) 30-253-4533
E-mail: jennesk@chem.uu.nl

Prof. Dr. P. W. Fowler, Dr. R. W. A. Havenith, A. Soncini,
Dr. E. Steiner
School of Chemistry, University of Exeter
Stocker Road, Exeter EX4 4QD (UK)
Fax: (+44) 1392-26-3434
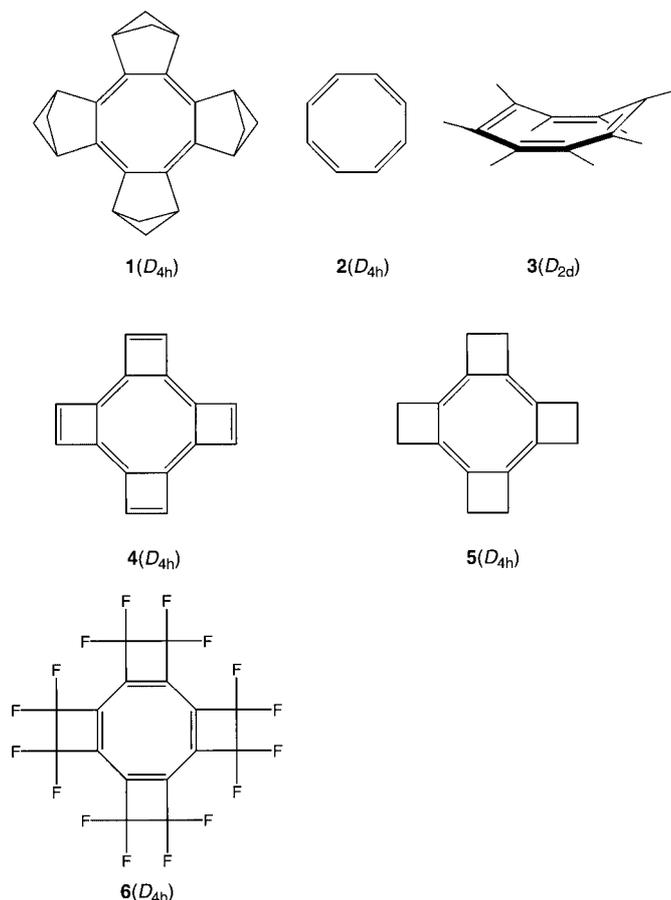
Scheme 1. Molecules under study.

ring current. Comparisons of currents in **1**(D_{4h}) with those in planar COT (**2**(D_{4h})), COT in its tub-shaped equilibrium geometry (**3**(D_{2d})) and COT moieties in hypothetical tetrakis(cyclobutadieno)- (**4**(D_{4h})) and tetrakis(cyclobuteno)cyclooctatetraene (**5**(D_{4h}), Scheme 1), will show that the choice of bridges used to effect clamping of COT into the plane determines whether or not a ring current exists.

Modern, distributed-origin, coupled Hartree–Fock methods such as the continuous transformation of origin of current density (CTOCD) method[16–19] are particularly suited for the visualization and interpretation of ring currents[20] (see Computational Section). Maps are shown in Figure 1 for the computed π-only and total ($\sigma + \pi$) current densities in **1**(D_{4h}). A strong, central paratropic ring current is evident in both
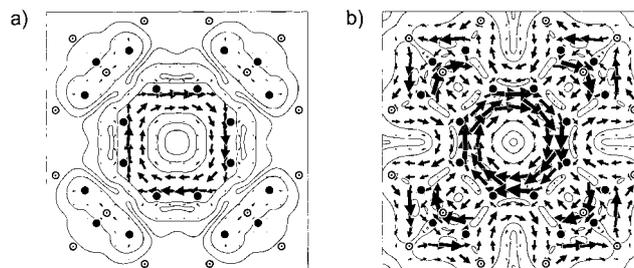
Figure 1. Maps of current density in tetrakis(bicyclo[2.1.1]hexeno)cyclooctatetraene (**1**): a) π-only, b) total ($\sigma + \pi$) current (● carbon, ○ hydrogen; nuclear positions projected in the plotting plane).

maps. The π contribution shows some variation in strength between alternate long and short bonds, which tends to equalize on inclusion of σ effects. Apart from the main paratropic ring current, some extraneous features arise in the total $(\sigma + \pi)$ map where the plotting plane cuts through the bridge bonds of the four bicyclo[2.1.1]hexeno units. However, the constrained COT subunit in this new molecule does indeed sustain the classical Hückel π current expected from its antiaromatic electron count. The question is whether this observation is a simple consequence of the enforced planarity of COT in **1**.

The answer is provided by the planar form of COT itself. On optimization in D_{4h} symmetry, the resulting closed-shell COT structure ($2(D_{4h})$), which is the transition state for tub-to-tub inversion,[21] exhibits bond alternation similar to that in the subunit of the stable molecule **1** (6-31G**: $\Delta R(\mathbf{1}) = 0.184$ Å, $\Delta R(\mathbf{2}) = 0.153$ Å). Planar COT (**2**) also displays the classical intense paratropic ring current expected for an antiaromatic π system (Figure 2a), associated here with the splitting into b_{2u} HOMO and b_{1u} LUMO in D_{4h} of the degenerate e_{2u} HOMO of the D_{8h} open-shell.[22] The reduced ring current of the stable molecule **1** is consistent with its larger HOMO–LUMO gap (**1**: 9.4 eV versus **2**: 8.5 eV).
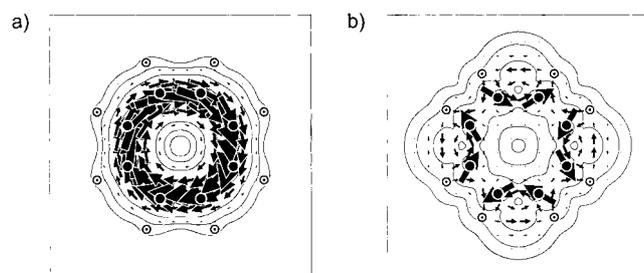
Figure 2. Maps of π-current density in a) planar COT (**2**), b) tub-shaped COT (**3**) (● carbon, ○ hydrogen; in (a) nuclear positions projected in the plotting plane. In (b) the median plane was used as the plotting plane).

Relaxation of COT to its tub-shaped equilibrium geometry **3** (D_{2d}) has little effect on the bond alternation (6-31G**: $\Delta R(\mathbf{3}) = 0.155$ Å) but destroys the delocalized ring current, as Figure 2b shows. Long and short bond lengths are similar for all three COT structures (**1**, X-ray averages 1.331(1)/1.500(1) Å; 6-31G** values: **1**(D_{4h}), 1.323/1.507 Å, **2**(D_{4h}), 1.326/1.479 Å, **3**(D_{2d}), 1.323/1.478 Å). The π-only map for **3** drawn in the median plane of the molecule shows localized circulations from the four double bonds, two above and two below the plotting plane. From this comparison of **2** and **3**, the importance of planarity is clear, notwithstanding previous literature statements,[12] but planarity alone is insufficient to ensure presence of a current, as the next example shows. In **4** (D_{4h}; see Scheme 1) the COT subunit is again clamped in the plane, in this case by annelation with rigid cyclobutadieno rings. In contrast to **1**, the π and total $(\sigma + \pi)$ maps for **4** (Figure 3) show the typical signature of localized double bonds. No paratropic π ring current is discernible in the COT unit of **4**, though the unsaturated four-membered cycles themselves support central (σ) paratropic contributions.

This quenching of the paratropic COT π current in **4** arises specifically from the conjugation of the clamping group with
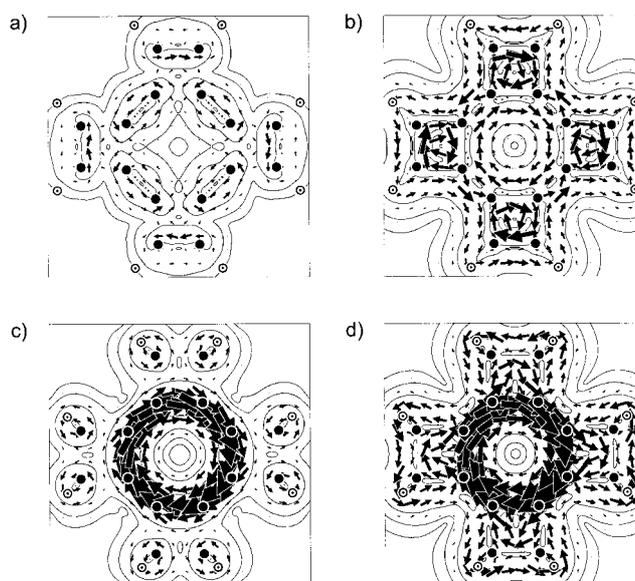
Figure 3. Maps of current density in tetrakis(cyclobutadieno)cyclooctatetraene (**4**) and tetrakis(cyclobuteno)cyclooctatetraene (**5**): a) π-only current in **4**, b) total $(\sigma + \pi)$ current in **4**, c) π-only current in **5**, and d) total $(\sigma + \pi)$ current in **5** (● carbon, ○ hydrogen; nuclear positions projected in the plotting plane).

the central ring. When the external π bonds of **4** are hydrogenated, to give the planar tetrakis(cyclobuteno) derivative **5** (D_{4h}), the COT paratropic current is restored (Figure 3c). The difference in current maps between **1**, **5** on the one hand and **4** on the other is evidently not a consequence of differences in bond alternation, (6-31G**: $\Delta R(\mathbf{4}) = 1.501 - 1.317 = 0.184$ Å, $\Delta R(\mathbf{5}) = 1.491 - 1.317 = 0.174$ Å). The explanation of the switch from localized to delocalized behavior lies instead in the difference between the π electronic structures of the 16-electron conjugated system in **4** and the eight-electron COT system in **1**, **2**, and **5**. As noted above, the planar COT ring has a b_{2u} HOMO and b_{1u} LUMO (Figure 4), and these are also HOMO and LUMO in **1** and **5**. The $b_{2u} \rightarrow b_{1u}$ occupied-to-virtual transition has the symmetry of a rotation about the magnetic field direction, and therefore produces a paratropic contribution.[22] This low-energy transition dominates the total π ring current and determines its paratropic sense. In **4** however, the interaction of the central COT π system (bonding orbitals a_{2u}, e_g, b_{2u}; antibonding b_{1u}, e_g, a_{1u}) with the four outer π bonds (bonding combinations a_{2u}, e_g, b_{1u}; antibonding b_{2u}, e_g, a_{1u}) pushes the occupied b_{2u} orbital down, below $2a_{2u}$ (HOMO – 1) and $2e_g$ (HOMO), and pushes the empty b_{1u} orbital up, above the $3e_g$ (LUMO) and $1a_{1u}$ (LUMO + 1) (Figure 4). The large paratropic $1b_{2u}$ orbital contribution is thereby suppressed and replaced by a mixture of weaker contributions ($2e_g \rightarrow 3e_g$ (paratropic), $2a_{2u} \rightarrow 3e_g$ (diatropic), $1b_{2u} \rightarrow 3e_g$ (diatropic)), which sum to localized diamagnetic circulations in the eight π bonds of **4**. In the language of reference [22], two-electron paramagnetism in **1**, **2**, and **5** has been replaced by eight-electron diamagnetism in **4**. This is a direct consequence of π–π interaction between COT and the clamping groups (see also references [23, 24]; if the *exo* single bonds of **4** are artificially stretched to 2 Å, for example, the central paratropic COT current reappears).
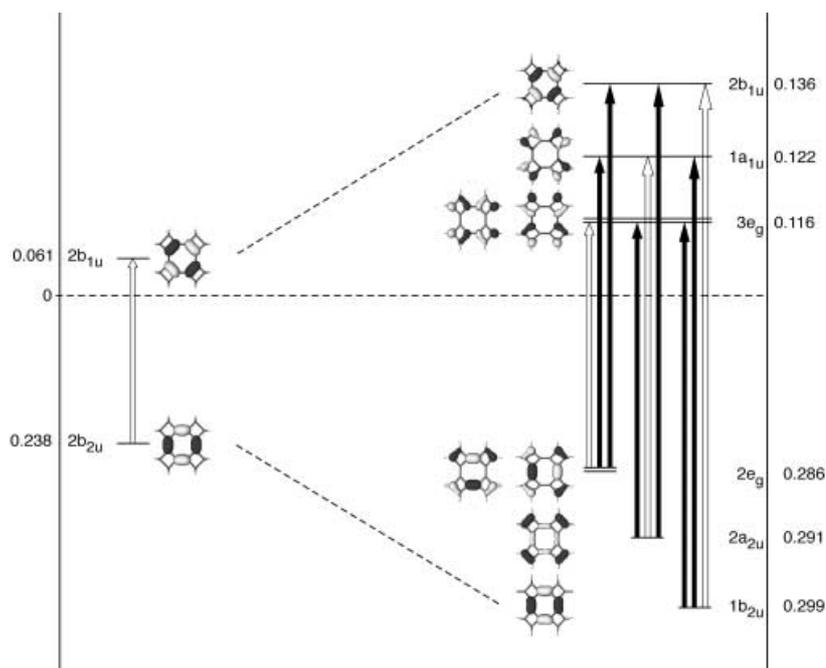
Figure 4. Three-dimensional contour maps of the HOMOs and LUMOs of **4** (right) and **5** (left), indicating their energies (Hartree) and symmetries. Black arrows represent translational transitions and white arrows rotational transitions from occupied levels.[22] The π molecular orbitals of **1** and **2** are similar to those of **5**.

method, where the current density at any point in space is calculated with that point as origin.[16–19] The method has the usual advantages of distributed-origin approaches: superior convergence with basis size and physically realistic current maps with modest basis sets (here 6–31G**). Optimized geometries, confirmed as minima (**1**, **3**–**6**) or in one case a transition state (**2**: one imaginary frequency), were computed in the same basis.

For all but **3** (see legend to Figure 2), current densities induced by a unit magnetic field acting along the principal axis are plotted in a plane 1 a_0 above that of the central ring (that is, close to the maximum π density and with current essentially parallel to the molecular plane, as shown previously[28]), the plotting area is 16×16 a_0^2, the contours denote the modulus of the current density, and the vectors represent in-plane projections of current. In all plots, diamagnetic circulation is shown anticlockwise and paramagnetic circulation clockwise.

The orbital picture also gives a ready explanation of the properties of other species such as perfluorinated tetrakis(cyclobuteno)cyclooctatetraene (**6**(D_{4h}), Scheme 1).[25] Replacement of H by F in **5** stabilizes the *endo* tautomer **6**,[12] but as this corresponds to a simple switch of HOMO and LUMO symmetries, the paratropic ring current should be retained. Explicit CTOCD-DZ calculations of current maps (not shown) confirm this expectation: **6** has indeed a strong central paratropic π current of similar intensity to that in **5**.

The series of calculations described here show that when COT is made planar, its magnetic response is essentially independent of the degree of bond alternation. A paratropic π ring current is compatible with clamping by groups that exert a purely geometrical effect. The crucial factor in the survival of the ring current is the rotationally allowed COT HOMO–LUMO transition; when interaction with the π system of an unsaturated clamping group opens up the gap between the b_{2u} and b_{1u} orbitals, the ring current is destroyed. In this context, the bicyclo[2.1.1]hexeno and cyclobuteno clamping groups are passive spectators, whereas the cyclobutadieno clamp actively suppresses the antiaromatic central current. The bicyclo[2.2.2]octene group[10] is also a spectator in this sense to a diamagnetic current in COT²⁻.

A parallel distinction in localization of central current is expected to apply to the equivalent derivatives of benzene.[6–9, 26]

Computational Section

Methods: The magnetic properties of all molecules were computed by using distributed-origin methods,[16, 17] at the coupled Hartree–Fock level,[18, 19] with the SYSMO program.[27] For the current–density maps, well-converged results are given by the DZ (diamagnetic zero) variant of the CTOCD (continuous transformation of origin of current density)

[1] F. London, *J. Phys. Radium* **1937**, *8*, 397–409.
[2] L. Pauling, *J. Chem. Phys.* **1936**, *4*, 673–677.
[3] J. A. Pople, *J. Chem. Phys.* **1956**, *24*, 1111.
[4] J. March, *Advanced Organic Chemistry*, Wiley, New York **1986**.
[5] For a general survey: M. Jones Jr., *Organic Chemistry*, Norton, New York, **2000**.
[6] N. L. Frank, K. K. Baldridge, J. S. Siegel, *J. Am. Chem. Soc.* **1995**, *117*, 2102–2103.
[7] H.-B. Bürgi, K. K. Baldridge, K. Hardcastle, N. L. Frank, P. Gantzel, J. S. Siegel, J. Ziller, *Angew. Chem.* **1995**, *107*, 1575–1577; *Angew. Chem. Int. Ed. Engl.* **1995**, *34*, 1454–1456.
[8] R. Diercks, K. P. C. Vollhardt, *J. Am. Chem. Soc.* **1986**, *108*, 3150–3152.
[9] D. Holmes, S. Kumaraswamy, A. J. Matzger, K. P. C. Vollhardt, *Chem. Eur. J.* **1999**, *5*, 3399–3412.
[10] K. Komatsu, T. Nishinaga, S. Aonuma, C. Hirosawa, K. Takeuchi, H. J. Lindner, J. Richter, *Tetrahedron Lett.* **1991**, *32*, 6767–6770.
[11] A. Matsuura, K. Komatsu, *J. Am. Chem. Soc.* **2001**, *123*, 1768–1769.
[12] K. K. Baldridge, J. S. Siegel, *J. Am. Chem. Soc.* **2001**, *123*, 1755–1759.
[13] P. von R. Schleyer, C. Maerker, A. Dransfeld, H. Jiao, N. J. R. van Eikema Hommes, *J. Am. Chem. Soc.* **1996**, *118*, 6317–6318.
[14] M. Pomerantz, R. N. Wilke, G. W. Gruber, U. Roy, *J. Am. Chem. Soc.* **1972**, *94*, 2752–2758.
[15] M. Christl, H. Reuchlein, *Angew. Chem.* **1990**, *102*, 1090–1091; *Angew. Chem. Int. Ed. Engl.* **1990**, *29*, 1035–1037.
[16] T. A. Keith, R. F. W. Bader, *Chem. Phys. Lett.* **1993**, *210*, 223–231.
[17] T. A. Keith, R. F. W. Bader, *J. Chem. Phys.* **1993**, *99*, 3669–3682.
[18] S. Coriani, P. Lazzeretti, M. Malagoli, R. Zanasi, *Theor. Chim. Acta* **1994**, *89*, 181–192.
[19] R. Zanasi, *J. Chem. Phys.* **1996**, *105*, 1460–1469.
[20] E. Steiner, P. W. Fowler, L. W. Jenneskens, *Angew. Chem.* **2001**, *113*, 375–379; *Angew. Chem. Int. Ed.* **2001**, *40*, 362–366.
[21] J. L. Andrés, O. Castaño, A. Morreale, R. Palmeiro, R. J. Gomperts, *J. Chem. Phys.* **1998**, *108*, 203–207.
[22] E. Steiner, P. W. Fowler, *J. Phys. Chem. A* **2001**, *105*, 9553–9562; E. Steiner, P. W. Fowler, *Chem. Commun.* **2001**, 2220–2221.
[23] R. Faust, E. D. Glendening, A. Streitwieser, K. P. Vollhardt, *J. Am. Chem. Soc.* **1992**, *114*, 8263–8268.
[24] K. K. Baldridge, J. S. Siegel, *J. Am. Chem. Soc.* **1992**, *114*, 9583–9587.
[25] F. W. B. Einstein, A. C. Willis, W. R. Cullen, R. L. Soulen, *J. Chem. Soc. Chem. Commun.* **1981**, 526–528.
[26] P. W. Fowler, R. W. A. Havenith, L. W. Jenneskens, A. Soncini, E. Steiner, *Chem. Commun.* **2001**, 2386–2387.
[27] P. Lazzeretti, R. Zanasi, SYSMO package (University of Modena), **1980**. Additional routines for evaluation and plotting of current density, E. Steiner, P. W. Fowler, unpublished results.
[28] A. Soncini, P. W. Fowler, I. Černušak, E. Steiner, *Phys. Chem. Chem. Phys.* **2001**, *3*, 3920–3923, and references therein.